



Experimental characterization of thermally-activated artificial muscles based on coiled nylon fishing lines

Antonello Cherubini, Giacomo Moretti, Rocco Vertechy, and Marco Fontana

Citation: *AIP Advances* **5**, 067158 (2015); doi: 10.1063/1.4923315

View online: <http://dx.doi.org/10.1063/1.4923315>

View Table of Contents: <http://scitation.aip.org/content/aip/journal/adva/5/6?ver=pdfcov>

Published by the [AIP Publishing](#)

Articles you may be interested in

[Fabrication and characterization of silver- and copper-coated Nylon 6 forspun nanofibers by thermal evaporation](#)

J. Vac. Sci. Technol. A **32**, 061401 (2014); 10.1116/1.4896752

[Multi-functional dielectric elastomer artificial muscles for soft and smart machines](#)

J. Appl. Phys. **112**, 041101 (2012); 10.1063/1.4740023

[Rotating turkeys and self-commutating artificial muscle motors](#)

Appl. Phys. Lett. **100**, 074108 (2012); 10.1063/1.3685708

[Experimental characterization and modeling of a nanofiber-based selective emitter for thermophotovoltaic energy conversion: The effect of optical properties](#)

J. Appl. Phys. **109**, 034306 (2011); 10.1063/1.3524567

[Thermal characterization of submicron polyacrylonitrile fibers based on optical heating and electrical thermal sensing](#)

Appl. Phys. Lett. **89**, 152504 (2006); 10.1063/1.2358952



Experimental characterization of thermally-activated artificial muscles based on coiled nylon fishing lines

Antonello Cherubini,¹ Giacomo Moretti,¹ Rocco Vertechy,²
and Marco Fontana^{3,a}

¹PERCRO SEES, TeCIP Institute, Scuola Superiore Sant'Anna, Pisa, Italy

²Department of Industrial Engineering, University of Bologna, 40126, Bologna, Italy

³ PERCRO SEES, TeCIP Institute, Scuola Superiore Sant'Anna, 56127, Pisa, Italy

(Received 1 April 2015; accepted 16 June 2015; published online 26 June 2015)

The discovery of an innovative class of thermally activated actuators based on twisted polymeric fibres has opened new horizons toward the development of effective devices that can be easily manufactured using inexpensive materials such as fishing lines or sewing threads. These new devices show large deformations when heated together with promising performance in terms of energy and power densities. With the aim of providing information and data useful for the future engineering applications, we present the results of a thermo-mechanical characterization conducted on a specific type of twisted polymeric fibre (i.e. nylon-made coiled actuators) that is considered particularly promising. A custom experimental test-bench and procedure have been developed and employed to run isothermal and isometric tensile tests on a set of specimens that are fabricated with a simple and repeatable process. The results of the experiments highlight some important issues related to the response of these actuators such as hysteresis, repeatability, predictability and stored elastic energy. © 2015 Author(s). All article content, except where otherwise noted, is licensed under a Creative Commons Attribution 3.0 Unported License. [<http://dx.doi.org/10.1063/1.4923315>]

I. INTRODUCTION

The last two decades have seen an increase of research and development activities on multifunctional materials to conceive lightweight, compact and low-cost actuators. In this context, materials such as Piezoelectrics,^{1,2} Magnetostrictive materials,³ Dielectric Elastomers (DEs),⁴ Carbon Nanotubes (CNTs),⁵ Shape Memory Materials^{6,7} are being investigated in a variety of applications, including robotics, micro electromechanical systems, process industry and energy harvesting. Most of these actuators based on multifunctional materials (such as DEs and piezoelectrics) are electrically or magnetically activated and in other cases, mechanical actuation is provided via a thermal energy input. The most well-known type of thermo-mechanical actuator is based on nickel-titanium alloys (namely, Shape Memory Alloys, SMAs) but also some kind of polymers⁹ have been studied for their capability to recover given deformation when heated above a certain temperature. Such a shape-memory effect is connected with a thermoelastic martensite-austenite phase transition in nickel-titanium alloys⁸ and with a variation of conformation entropy in shape memory polymers.¹⁰

Recently, Haines et al.¹¹ discovered a new class of thermo-mechanical actuators made out of drawn polymeric fibres, commonly employed as fishing lines and sewing threads. Specifically, the authors of this work demonstrated that certain polymers (most notably nylon) experiment relevant temperature-induced deformations if their fibres are properly twisted and eventually coiled, and they can be employed both as linear or rotational actuators. This new Twisted-Polymeric-Fibre Actuators (TPFA) show outstanding performances such as energy densities as high as 2.63 kJ/kg and power densities over 5.3 kW/kg, with strokes up to 50%. These properties, together with the

^aElectronic mail: m.fontana@sssup.it



ease of manufacturing and the extremely reduced cost of the employed materials (e.g. monofilament nylon fibres are sold at a retailer price of about 160 \$/kg, comparing to around 3600 \$/kg for SMA wires), make these new actuators an extremely promising technology. Possible future applications of TPFA may include: linear and torsional actuators, chemically activated thermal actuators, solar trackers, vibration dampers, biomedical actuators, energy harvesting devices, waste heat recovery devices, actuated fitting garment and textiles.¹²

At the present stage, the basic principle of TPFA have been demonstrated but further investigations are required to enable their application in practice. Specifically, load-deformation response of twisted and coiled yarns must be known in a wide range of temperatures and in different loading conditions and performance parameters of hysteresis and repeatability have to be assessed. Moreover, important aspects such as fatigue, ageing and lifetime have to be fully characterized in order to practically evaluate potential implementations of machines based on TPFA.

In this context, this work has been conducted to shed some light on a few of the above-mentioned unexplored aspects. Specifically, in this paper we provide an experimental characterization for a type of TPFA based on nylon wires. A purposely developed setup has therefore been built and a quite repeatable manufacturing procedure for actuators is proposed. Isothermal and isometric responses (which are new in literature) are measured over a wide range of deformation. These measurements, that are acquired during loading and unloading, make it possible to observe and evaluate hysteresis (and its dependence upon temperature) together with other interesting aspects such as: (1) an inverted behaviour in temperature response recorded above certain strains; (2) a very repeatable and predictable force vs temperature output in isometric tests. Moreover, the acquired isothermal response makes it possible to evaluate the performance of TPFA employed as simple passive mechanical spring, showing very promising performances in terms of capability of storing elastic energy.

The paper is organized as follows. In section II the working principle of TPFA is briefly illustrated, in section III the test-bench and the specimen preparation are described, and finally section IV shows the results of the performed thermo-mechanical tests, including isothermal and isometric tests.

II. ACTUATION PRINCIPLE

The working principle of TPFA is based an extremely simple phenomenon that is connected with expansion or contraction of a twisted polymeric fibre in longitudinal or radial directions. Specifically, it can be geometrically demonstrated^{13,14} that twisted fibres partially untwist as their diameter expands or their longitudinal axis contracts. Thus, two contributions of “thermal untwist” can be obtained: one due to a positive radial thermal expansion coefficient and one due to a negative axial expansion coefficient. This effect can be directly exploited to obtain torsional actuators. Alternatively, linear actuators can be obtained by coiling the twisted fibres.

Thermal actuation can be provided by using air or water flows at controlled temperature, or by Joule heating thanks to the application on the coil of metallic coatings, paints or wires.

TPFA are obtained by a simple manufacturing process that starts from a virgin polymeric wire (here after called precursor fibre). To date, extruded wire made of nylon 6, nylon 6.6, polyethylene, kevlar, polyvinylidene fluoride (PVDF), and polyester have been tested.¹¹ To obtain a TPFA, the precursor fibre is “twisted”, i.e. one of its ends is turned several times with respect to the other around its longitudinal direction. After such twisting procedure, the fibre can be arranged in different configurations to obtain: torsional or linear actuator. Specifically, a twisted fibre can be kept in its original cylindrical shape to obtain torsional actuators or can be “coiled” (i.e. the central axis of the wire assumed the shape of a helix with constant pitch) to obtain linear actuators. In both cases, a thermal treatment is employed to stabilize the final twisted (and eventually coiled) shape.

As shown in Figure 1, the coiling required for linear actuators can be homochiral, (i.e. coiling and twisting have the same chirality) or heterochiral (i.e. coiling and twisting have opposite chirality). An increase in temperature generates a contraction of the actuator in the first case and an expansion in the second case.

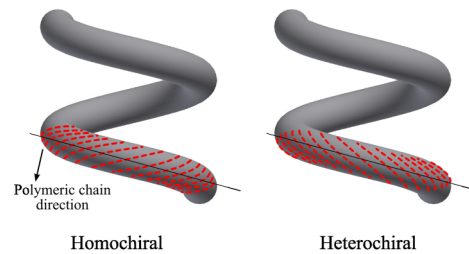


FIG. 1. Schematic representation of homochiral and heterochiral coiled TPFA fibers. Polymeric chain direction is highlighted in red.

Coils can be obtained using two procedures:

- Autocoiling: by inserting in the precursor fibre (i.e. the untwisted nylon wire) a large amount of twist so that coils are generated due to a mechanical instability,
- Mandrel coiling: by wrapping the twisted fibre around a mandrel.

Coils produced by autocoiling are always homochiral, while mandrel coiling makes it possible to obtain both homochiral and heterochiral coils.

The thermo-mechanical response of a TPFA depends on several factors: 1) precursor fibre diameter; 2) coil index, C , defined as the ratio of the average coil diameter divided by the precursor fibre diameter; 3) unloaded coil bias angle, α_c , formed by the coiled fibre with an axis perpendicular to the coil longitudinal direction (see Figure 4).

Haines *et al.*¹¹ investigated the influence of such geometric parameters on the actuators performance. Specifically, coils with index C ranging from 1.1 to 5.5 have been tested. It was observed that TPFA fibers with small coil index are stiffer, provide larger actuation forces and reach higher energy densities, nonetheless they provide limited stroke. On the other hand, TPFA fibers featuring large coil index show larger actuation strokes, but smaller stiffness, load capacity and energy density. Actuators made of polyethylene experiments larger tensile actuations in response to a unit temperature variation, but are able to work in a limited temperature range because of the lower melting point. Nylon 6 and nylon 6.6 were demonstrated to be the most suitable materials for these applications having the largest melting temperature and tensile strokes.

In the following sections of this paper, we focus on a specific fibre made of Nylon 6 that is employed to produce homochiral actuators by autocoiling. We made this choice since we consider that this type of TPFA could be one of the most promising, thanks to the combination of the low-cost material and the ease of manufacturing.

III. EXPERIMENTAL SETUP

In this section, we focus on homochiral nylon actuators produced by autocoiling (hereafter referred as nylon coils or simply NC), which are the object of the experimental tests discussed in this paper. In order to be properly characterized, NC specimens have to be experimentally tested over a wide range of temperatures in presence of large deformations. For this reason, a testing machine for the characterization of NCs has been purposely built in order to perform tensile tests at controlled programmable temperatures.

A. Test bench

The machine is composed by an upper and a lower assembly (see Figure 2-right) on which the ends of the specimens are respectively attached. The upper assembly is fixed to the main frame while the lower one can slide linearly along the vertical direction. The assemblies have two coaxial glass cylinders that are arranged to form an open air duct through which hot air flows (see Figure 2-left). The motion is provided by a linear motor (LinMot HS01-37 × 166). The position is measured through an integrated magnetic encoder and the force is acquired through a monoaxial

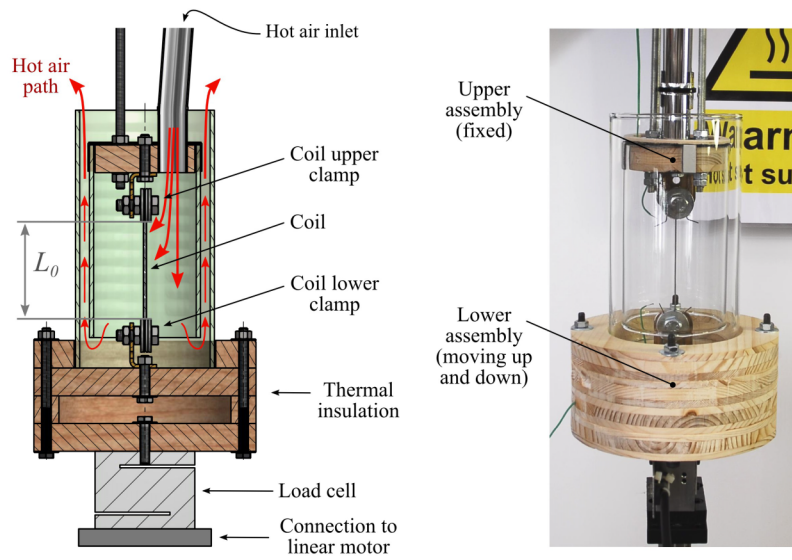


FIG. 2. Schematic and photograph of the test bench in the configuration with unstretched coil.

load-cell (DS Europe 535 QD A1). In order to prevent the load-cell from overheating (the maximum operating temperature for the load cell is 40 °C) the lower assembly includes an insulating wall made of alternating wood and air layers.

The operation of the testing machine is schematically depicted in Figure 2. The hot air flow enters the upper assembly and follows a path such that the whole length of the coil is invested by the air stream. The turbulence of the flow guarantees homogeneous temperature. Two thermocouples, located in different points of the chamber, allow to verify the homogeneity of the temperature. The setup features a maximum stroke of 160 mm, maximum force of 250 N and can reach temperatures high as 200 °C with an uncertainty of ± 5 °C. The test-bench is designed to host specimens with variable initial length and strokes.

B. Specimen preparation procedure

An easy and repeatable autocoiling manufacturing process is employed to produce the NC specimens.¹⁴ Coiled actuators are obtained from the precursor fibre (i.e. initial untwisted nylon wire) by connecting its top end to a rotating motor and the bottom end to a suspended mass that keeps the wire tensioned at constant force. The bottom of the wire is prevented from rotation around the vertical axis (see in Figure 3) thus every turn of the motor adds one turn of twist to the fibre. In a prescribed range of tensions, after several turns, the wire starts to buckle and assumes a coiled shape. With the same precursor fibre, different coil shapes (with different coil indexes) can be obtained by varying the value of the tension during twisting. Higher production loads originate coils with smaller coil index.

Right after the twisting and coiling process, the NC is fixed to a frame that prevents the fibre from untwisting or losing its shape when the weight is removed. The coil (together with the frame) is exposed to heat treatment in air and then removed from the frame (without losing twist).

IV. EXPERIMENTAL TESTS

In this section we report a set of experiments conducted on a homochiral Reference Coil (RC), manufactured according to the procedure illustrated in Section III B. A nylon 6 monofilament (Teklon Carson fishing line) with diameter of 0.5 mm was used as precursor fibre. The RC was manufactured using a load of 0.5 kg, i.e. a “nominal stress” of 25 MPa, defined as the ratio of the applied load over the cross section of the untwisted precursor fibre. The RC (depicted in Figure 4)

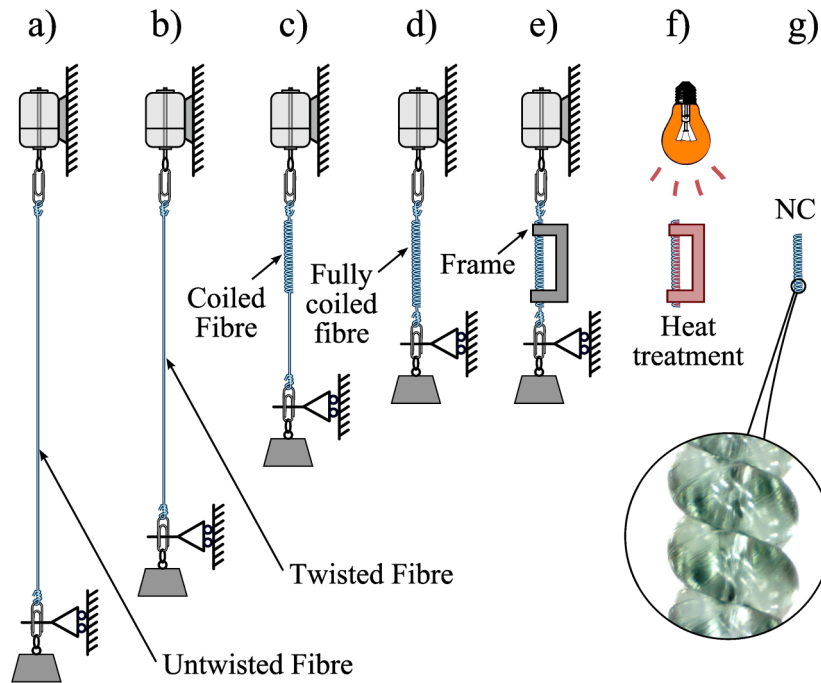


FIG. 3. Scheme of the autocoining process for NC: a) The precursor fibre has the top end fixed to a motor, and the bottom end rigidly attached to a weight which is prevented from rotation and is free to slide up and down. b) As the motor starts rotating, the fibre is twisted. The fibre visibly shortens. c) Coiling is generated by mechanical instability (autocoining). d) When the whole length is coiled, the motor is stopped. e) The NC is fixed on a rigid frame. f) A heat treatment fixes the shape. g) The NC is ready.

was subjected to 1-hour on-frame thermal annealing in air at 150 °C. The “nominal length” of the RC (defined with respect to the equilibrium configuration in which no loads are applied to the coil ends, at ambient temperature) is $L_0 = 70$ mm, and its mass is 75.6 mg. The precursor untwisted fibre length was about 4.4 times the nominal length. Coil index and bias angle, measured after the heat treatment, in the unstretched configuration, are $C = 1.4$ and $\alpha_c = 18^\circ$ respectively. Prior to the mechanical tests, the RC was subjected to four loading cycles at 122 °C temperature and 50% of deformation (i.e. the maximum temperature and elongation that are employed in the subsequent tests), in order to set any eventual permanent modification due to the combined effect of strain and temperature.

Deformation is defined as the ratio between the increase in coil length ΔL (mm) (with respect to the nominal length) and the nominal length, L_0 , itself.

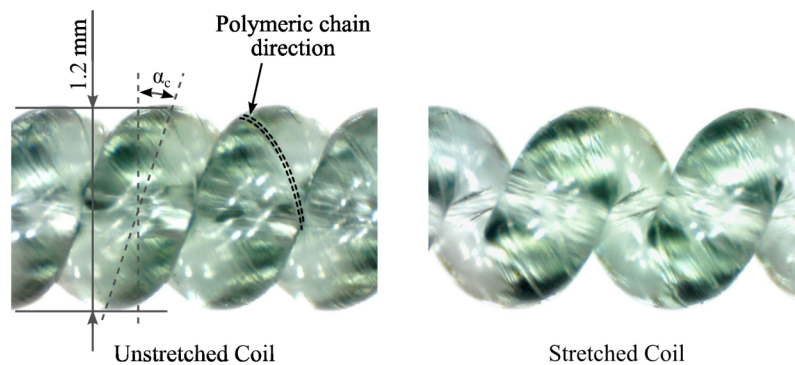


FIG. 4. Microscope photographs of the NC: coil in the unstretched (top) and stretched (bottom) configuration. Circular light patterns are the reflections of the microscope LEDs.

A. Isothermal tests

Cyclic tensile tests at constant temperature were performed imposing $\Delta L = 35$ mm, i.e. 50% of the nominal length of the specimen. This strain was conservatively chosen basing on preliminary rupture tests made on a series of RCs, which experimented rupture approximately at 110-120% strain at ambient temperature. Tensile tests were repeated at four different temperatures, from 25 °C (ambient temperature) to 122 °C, spaced approximately 30 °C apart. Temperatures are here expressed as the time average of the measured time profiles, which are approximately constant within a range of ± 5 °C with respect to the average value.

In order to set an appropriate deformation rate, preliminary tests have been conducted between $14.3 \cdot 10^{-3} \text{ s}^{-1}$ and $71.4 \cdot 10^{-3} \text{ s}^{-1}$ (i.e. 1 mm/s and 5 mm/s, respectively) concluding that results were not affected by the choice. Thus, a deformation rate of $28.6 \cdot 10^{-3} \text{ s}^{-1}$ (i.e. 2 mm/s) has been selected as a trade-off between noisy measurements and long time-consuming tests that would have occurred with the choice of high and low rates, respectively. The deformation time-history, for each temperature, is composed by ten loading cycles described as follows:

- the RC is stretched from L_0 to the maximum deformation at the selected deformation rate;
- the coil is kept at the maximum deformation (i.e. 50%) for 2 s;
- the RC length is then reduced down to the unstretched configuration, at the selected deformation rate;
- the coil is kept at the nominal length for 2 s, then the cycle is repeated.

The isothermal load-deformation curves are reported in Figure 5. The plots show an hysteretic behaviour of the RC, with a response that becomes repeatable after approximately one training cycle.

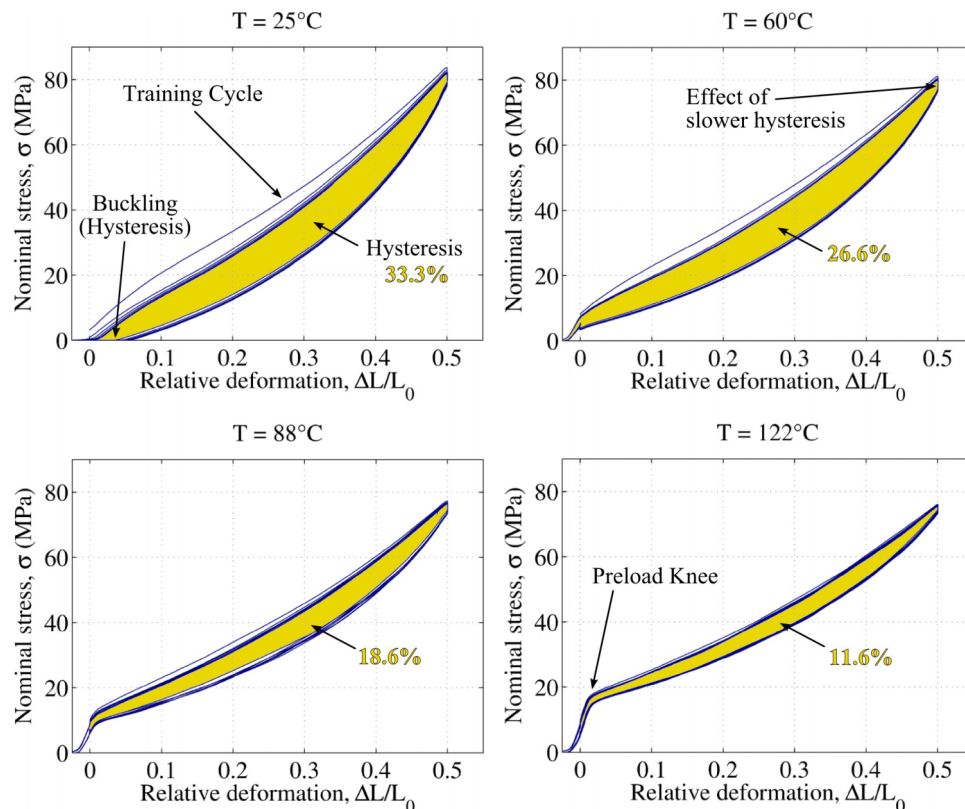


FIG. 5. Cyclic tensile tests at 4 different temperatures.

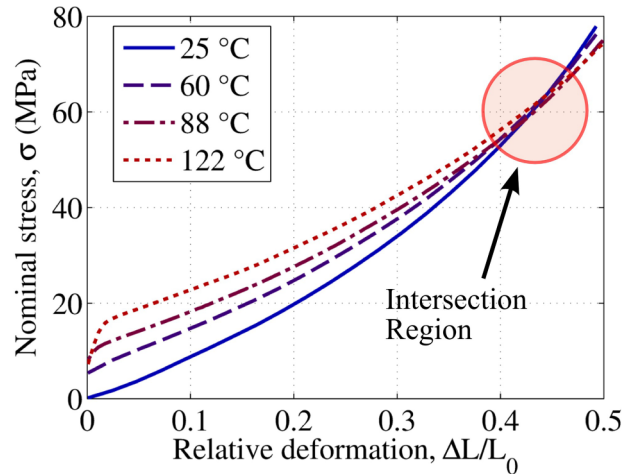


FIG. 6. Experimental average stress-deformation responses at different temperatures.

Observing the curves shown in Figure 5, the following considerations can be outlined:

- Hysteresis losses decrease with increasing temperature. This same behaviour has been detected on other polymeric materials.^{15,16} Figure 5 reports the percentage of hysteresis losses at different temperatures, calculated on the average response over the last two loading cycles and expressed as the amount of dissipated energy over the elastic energy provided to the sample during the stretching phase.
- As temperature increases, the curves show an increasing steep segment (here referred to as preload knee) at small deformations ($\Delta L/L_0 < 0.02$), i.e. the specimen presents much higher stiffness at low stretches. This is because the coils start touching each other.
- At higher temperatures, the first training cycle is closer to the stabilized response.
- When the RC is kept for 2 s at 50% deformation, slower hysteresis phenomena induce a slight stress relaxation (see Figure 5).
- Due to hysteresis, during the unloading phase of isothermal tensile cycles at 25 °C, the sample suffers from buckling, i.e. its stress falls to zero, as it approaches the reference configuration.

The responses of the RC averaged on loading and unloading cycles are shown in Figure 6 for different temperatures. For deformations up to 40 %, the higher the temperature, the higher the mean force exerted by the RC in correspondence of a given strain. The loading curves at the different temperatures mutually intersect in a tight region around 45 % strain and 60 MPa nominal stress. For larger strains, the behaviour of the force with respect to the temperature is the opposite, i.e. for very large values of the stress (and, thus, of the strain), the NC tends to extend when temperature is increased. Notice also that the slopes of the curves are different. This means that it is possible to control the stiffness of the actuator by varying the temperature. For example, for a deformation $\Delta L/L_0 = 0.07$ a stiffness of 101 MPa or 78 MPa can be obtained with a temperature of 25 °C or 122 °C, respectively. This feature can be useful in a number of applications, e.g. vibration control.

B. Isometric tests

Isometric tests have been conducted using constant elongations of 10, 15 and 20 mm respectively (i.e. deformations of 14.3 %, 21.4 % and 28.6 %). The corresponding results are hereafter referred to as datasets A, B and C respectively. These deformation values are well below the intersection region of Figure 6. The RC was subjected to thermal cycles starting from ambient temperature of 24 °C up to 120 °C, with a temperature variation rate was approximately 0.13 °C/s (both in rising and descending). In each experiment, the specimen was subjected to two consecutive thermal cycles, the first of which has been considered a training cycle to obtain a repeatable

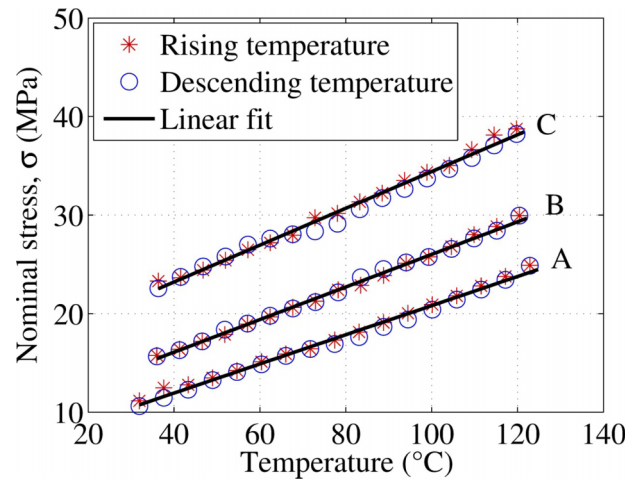


FIG. 7. Stress vs. temperature measured for three isometric tests at 14.3 % (dataset A), 21.4 % (dataset B) and 28.6 % (dataset C) deformation.

isometric behaviour. The reported results refer to measurements obtained during the second thermal cycle. Nominal stress profiles as functions of temperature for the three datasets are depicted in Figure 7. Measurements taken during the rising of temperature and during the decreasing of temperature are indicated with different markers (asterisks and circles respectively).

We can observe that:

- As expected, force increases with rising temperature.
- There is no substantial distinction between the force-temperature measurements from rising temperature and descending temperature curves.
- The dependence of the produced load over the temperature appears very linear.

Fitting each dataset to a linear function, as in Eq. (1)

$$\sigma = \alpha T + \beta, \quad (1)$$

yields the coefficients given in Table I.

Figure 8 reports the experimental nominal stress and the test-bench chamber temperature variations over time for the second thermal cycle of dataset B. As shown, the coil rapidly responds to temperature variations, thanks to its low thermal capacitance. Moreover, the force output is very sensitive to small temperature variations. Green circles in Figure 8 represent the estimated load as a function of the measured temperature for dataset B, calculated using the linear fitting parameters of Table I. Similar results hold for datasets A and C. The high repeatability and linearity of isometric response make NCs application promising in applications where they are employed as controlled force actuators in a fixed configuration.

C. Mapping of the mechanical response

In this section, we compare the results from isothermal cyclic tensile tests and isometric tests. If the mechanical (stress-strain) response of a NC specimen was fully repeatable, data obtained

TABLE I. Linear fitting coefficients for the data of Figure 7.

Dataset	Elongation (%)	α (MPa/°C)	β (MPa)
A	14.3	$1.48 \cdot 10^{-1}$	6.02
B	21.4	$1.65 \cdot 10^{-1}$	9.47
C	28.6	$1.87 \cdot 10^{-1}$	15.73

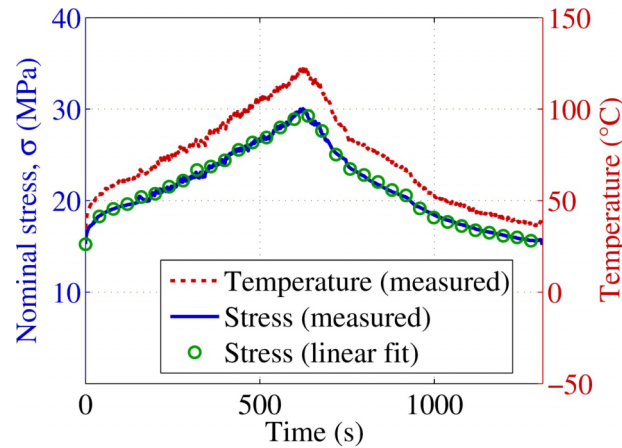


FIG. 8. Time plot of the measured temperature and nominal stress during isometric thermal cycle (dataset B). Red-dotted line shows the temperature, blue-solid line represents the measured stress, while green circles represent the stress predicted by Eq. (1).

from the two sets of tests (and relative to the same temperature and deformation) would overlap. Nonetheless, due to hysteresis, thermal settling of polymers, and memory effects in general, it is reasonable to expect that these actuators behave slightly differently when subjected to different loading mechanisms. In Figure 9-left, the mean isothermal curves are superimposed with the points representing the interpolated measured stress at the four reference temperatures (25-60-88-122 °C) for the three isometric datasets. The load measured in isometric conditions is always lower than the corresponding average isothermal load, with differences up to 30% at 25 °C. Nonetheless, if isometric measurements are compared with the unloading isothermal curves (Figure 9-right), a much better agreement is obtained.

Beyond the numerical information and the estimate of the involved orders of magnitude, the characterization of Figure 9 is a useful tool which also provides qualitative information about the different response of NC actuators in diverse tests, other than isotonic experiments already described in Ref. 11.

It is possible to roughly estimate the maximum mechanical work that can be performed by a NC that works in a fixed temperature range by calculating the area enclosed by the mean isothermal curves corresponding to the two extreme temperatures of the range. For the chosen RC and working conditions (temperature between 25 °C and 122 °C), a maximum of 0.8 kJ/kg has been recorded. Nonetheless, as the NC has a memory behaviour which makes its response dependent on the past

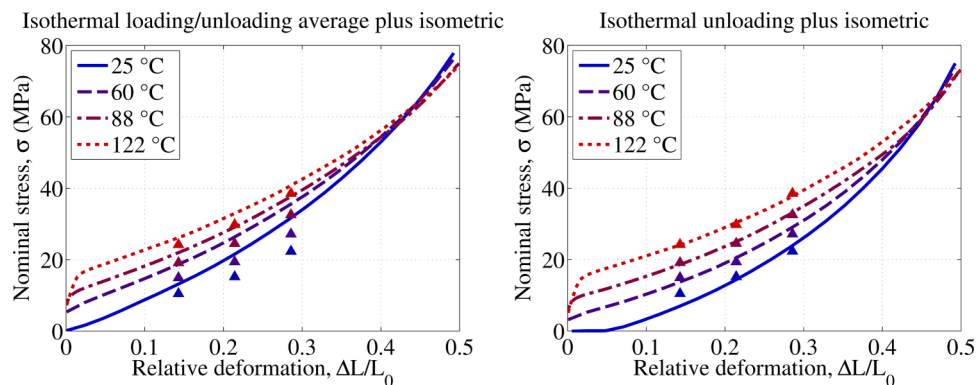


FIG. 9. Experimental characterization of the RC mechanical response. The lines represent the average response in cyclic isothermal tests. Triangular markers represent the interpolated force in isometric tests, at the same temperatures at which isothermal tests were conducted.

TABLE II. Stored elastic energy density (relative to an isothermal extension of the NC sample) and hysteresis losses for the different tensile isothermal tests at 50% deformation.

Temperature (°C)	Energy Density (kJ/kg)	Hysteresis losses (%)
25	3.32	33.3
60	3.57	26.6
88	3.61	18.6
122	3.77	11.6

loading history, an exact estimation of this mechanical work could be provided with an experiment in which the maximum energy actuation cycle is measured while properly adjusting the load and the temperature.

D. Estimation of elastic energy

The evaluation of the maximum elastic energy that can be stored in nylon coils is interesting to evaluate their possible application as springs. Steel springs have elastic energy densities up to 0.9 kJ/kg, assuming that the material is uniformly deformed to the breaking load.¹⁷ Driven by data already provided for existing non-coiled nylon springs (up to 2.1 kJ/kg¹⁷), we performed a series of tests to assess the potential of coiled nylon springs.

We started with an experimental assessment of straight, non-twisted, non-coiled, monofilament nylon 6 fibre used as a precursor of the RC. We measured a breaking stress of 924 MPa and an average elastic modulus of 3.3 GPa at ambient temperature, thus yielding and energy density higher than 100 kJ/kg. Nonetheless, handling the untwisted precursor fibre to store elastic energy may not be convenient in many technical applications because of the small deformation and the high stiffness.

In Table II, the elastic energy density of springs made of NCs is calculated as the elastic energy provided to the RC during the stretching phase of the isothermal tests in Figure 5. Values larger than those in Table II may be obtained considering a wider deformation range, up to the breaking condition. For instance, an average value of 11 ± 2 kJ/kg has been obtained testing six specimens (manufactured as the RC) at breaking conditions (124 MPa nominal stress and 112% deformation at room temperature).

All the measured values for nylon springs are far larger than the maximum energy density of steel springs and they exceed previous data on nylon springs. Nonetheless, in order to apply nylon springs in real frameworks, other aspects should be considered, such as the limitations related to the relevant hysteresis losses.¹⁷

V. CONCLUSIONS

This article investigates a novel category of thermo-mechanical actuators based on twisted and coiled polymeric fibres. These actuators have the capability of responding to temperature variations producing a large amount of untwisting and a resulting variation in longitudinal length.

Among the possible materials and configurations, we have focused on Nylon 6 coiled actuators (called nylon coils or more simply NC) that are obtained through a simple autocoiling process.

Thanks to a tailor-made experimental setup, isothermal and isometric tests have been conducted at different temperatures, up to approximately 120 °C. The acquired and elaborated data in this work allow to observe specific phenomena which were not identifiable on the basis of previous literature results, such as:

- Hysteresis in mechanical response:
Detailed and multi-temperature isothermal tests on NCs are presented here for the first time. Such results clearly show that a NC features a consistent amount of hysteresis losses and that hysteresis depends highly on temperature, decreasing at higher temperatures (Section IV A).

- Isothermal curves intersection:
Isothermal tests have shown that, when highly strained, coiled actuators revert their tendency to shorten/extend with increasing temperature (section IV A).
- Isometric temperature-load profiles:
Isometric measurements show a highly repeatable response of NCs load variations to temperature change, with a clearly linear trend (section IV B).
- New data about elastic energy densities:
Stored elastic energy have been measured and show that coiled actuators could be successfully employed as high performance passive springs.

Future works may address other unexplored areas such as: comparisons among different crystallinity and types of precursor fibres (i.e. nylon 6.6 and polyethylene), assessments of the influence of some manufacturing parameters (e.g. load during fabrication, heat treatment temperature, thermal annealing in air or vacuum) on the mechanical response and on the energy density, dynamic behaviour, etc. Future work should also investigate some possible critical aspects such as durability, fatigue lifetime, UV resistance, or effect of hygroscopy on the performance.

ACKNOWLEDGMENTS

This research is funded by Scuola Superiore Sant'Anna under grants I6014MF (Principal Investigator: Marco Fontana) and I6014RV (Principal Investigator: Rocco Vertechy).

- ¹ H. Jaffe and D. A. Berlincourt, "Piezoelectric transducer materials," *Proceedings of the IEEE* **53**(10), 1372-1386 (1965).
- ² B. Jaffe, *Piezoelectric ceramics* (Academic Press Inc. Ltd, London, 1971).
- ³ F. Claeysen, N. Lhermet, R. Le Letty, and P. Bouchilloux, "Actuators, transducers and motors based on giant magnetostrictive materials," *Journal of Alloys and Compounds* **258**(1), 61-73 (1997).
- ⁴ F. Carpi, D. De Rossi, R. Kornbluh, R. E. Pelrine, and P. Sommer-Larsen, *Dielectric elastomers as electromechanical transducers: Fundamentals, materials, devices, models and applications of an emerging electroactive polymer technology* (Elsevier Ltd, Amsterdam, 2008).
- ⁵ R. H. Baughman, C. Cui, A. A. Zakhidov, Z. Iqbal, J. N. Barisci, G. M. Spinks, G. G. Wallace, A. Mazzoldi, D. De Rossi, A. G. Rinzler, O. Jaszinski, S. Roth, and M. Kertesz, "Carbon nanotube actuators," *Science* **284**(5418), 1340-1344 (1999).
- ⁶ K. Otsuka and C. M. Wayman, *Shape memory materials* (Cambridge University Press, Cambridge, 1999).
- ⁷ K. Ullakko, "Magnetically controlled shape memory alloys: a new class of actuator materials," *Journal of materials Engineering and Performance* **5**(3), 405-409 (1996).
- ⁸ T. Tadaki, K. Otsuka, and K. Shimizu, "Shape memory alloys," *Annual Review of Materials Science* **18**(1), 25-45 (1988).
- ⁹ C. Liu, H. Qin, and P. T. Mather, "Review of progress in shape-memory polymers," *Journal of Materials Chemistry* **17**(16), 1543-1558 (2007).
- ¹⁰ P. T. Mather, X. Luo, and I. A. Rousseau, "Shape memory polymer research," *Annual Review of Materials Research* **39**, 445-471 (2009).
- ¹¹ C. S. Haines, M. D. Lima, N. Li, G. M. Spinks, J. Foroughi, J. D. Madden, S. H. Kim, S. Fang, M. J. De Andrade, F. Göktepe, Ö. Göktepe, S. M. Mirvakili, S. Naficy, X. Lepr, J. Oh, M. E. Kozlov, S. J. Kim, X. Xu, B. J. Swedlove, G. G. Wallace, and R. H. Baughman, "Artificial muscles from fishing line and sewing thread," *Science* **343**(6173), 868-872 (2014).
- ¹² N. Li, C. S. Haines, M. D. Lima, M. Jung de Andrade, S. Fang, J. Oh, M. E. Kozlov, F. Göktepe, Ö. Göktepe, D. Suh, and R. H. Baughman, "Coiled and non-coiled twisted nanofibre yarn and polymer fibers torsional and tensile actuators," Patent WO2014022667 (A2) (2014).
- ¹³ S. M. Mirvakili, A. R. Ravandi, I. W. Hunter, C. S. Haines, N. Li, J. Foroughi, S. Naficy, G. M. Spinks, R. H. Baughman, and J. D. W. Madden, "Simple and strong: Twisted silver painted nylon artificial muscle actuated by Joule heating," *SPIE Smart Structures and Materials + Nondestructive Evaluation and Health Monitoring* (International Society for Optics and Photonics, 2014).
- ¹⁴ G. Moretti, A. Cherubini, R. Vertechy, and M. Fontana, "Experimental characterization of a new class of polymeric-wire coiled transducers," *SPIE Smart Structures and Materials + Nondestructive Evaluation and Health Monitoring* (International Society for Optics and Photonics, 2015).
- ¹⁵ K. K. Kar and A. K. Bhowmick, "High-strain hysteresis of rubber vulcanizates over a range of compositions, rates, and temperatures," *Journal of applied polymer science* **65**(7), 1429-1439 (1997).
- ¹⁶ T. Rey, G. Chagnon, J. B. Le Cam, and D. Favier, "Influence of the temperature on the mechanical behaviour of filled and unfilled silicone rubbers," *Polymer Testing* **32**(3), 492-501 (2013).
- ¹⁷ M. F. Ashby, *Materials selection in mechanical design* (Pergamon Press, Oxford, 1992), Chapters 6, 7.